Role of imaging in diagnosis of abdominal angina

Essay

Submitted for partial fulfillment of master degree of radiodiagnosis

By

Alsayed Hussein Mohammad Alsayed

(M.B., B.CH)

Under Supervision Of

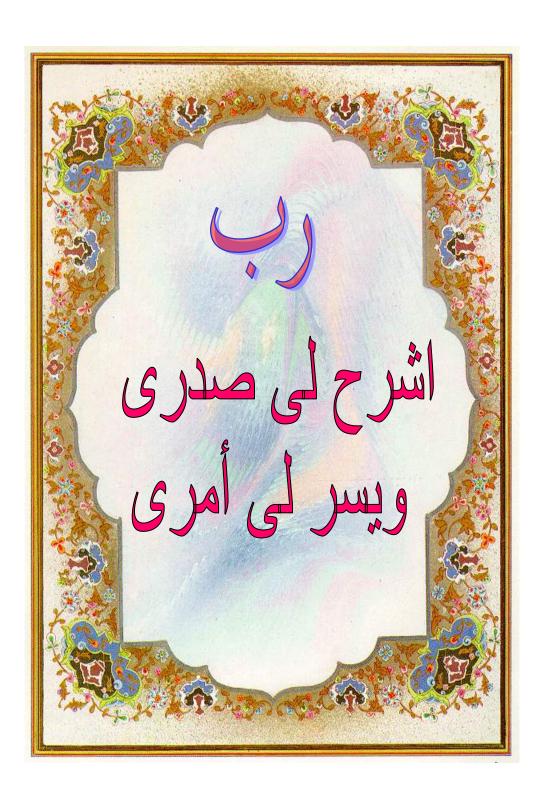
Prof. Dr/ Ola Mohammad Gamal Eldine Nouh

Professor of Radiodiagnosis
Faculty of medicine, Ain-Shams University

Prof. Dr/ Samer Malak Boutros

Assistant professor of Radiodiagnosis
Faculty of medicine, Ain-shams University

Faculty of Medicine
Ain-Shams University
2010



<u>Acknowledgment</u>

First of all thanks to Allah

Words do fail me when I come to express my sincere appreciation to Prof. Dr. Ola Mohammad Gamal Eldine, professor of Radiodiagnosis, Faculty of Medicine, Ain Shams University, for her great help, constructive criticism and kind supervision. No word can fulfill the feeling of gratitude and respect I carry for her.

Special thanks are due to Prof. Dr. Samer Malak Boutros,
Assistant professor of Radiodiagnosis, Faculty of Medicine,
Ain Shams University, for his valuable help and close step
by step guidance all through this work, and to whom I pay
my full regards for the great effort and full assistance that
he generously offered me.

Lastly, but not least; I would like to thank my Dear Family for their support and continuous encouragement and to whom I pay my full credit to all success I may have yielded and success yet to come, and for whom I wouldn't have this work accomplished without them.

Alsayed Hussein

List of contents

List of abbreviation	
List of figures	IV
List of tables	X
Introduction	1
Aim of the work	4
Anatomy	5
Pathology	28
Technique	44
Findings with illustrations	145
Summary and conclusion	190
References	197
Arabic summary	ĺ

List of Abbreviations

2D	Two-dimensional
3D	Three-dimensional
AA	Abdominal angina
AEC	Automatic exposure control
AI	Acceleration index
AO	Aorta
AT	Acceleration time
CA	Celiac artery
CE	Contrast enhanced
CFA	Common femoral artery
CIA	Common iliac artery
CIN	Contrast-induced nephropathy
CMI	Chronic mesenteric ischemia
CPR	Curved planar reformation
CTA	Computed tomographic angiography
DSA	Digital subtraction angiography
DSCT	Dual-source CT
EDV	End-diastolic velocity
FDA	Food and drug administration
FMD	Fibromuscular dysplasia
FSE	Fast spin-echo
FSPGR	Fast spoiled gradient-echo
Gd	Gadolinium
GE-MRA	Gadolinium enhanced magnetic resonance angiography

GRE	Gradient echo
IMA	Inferior mesenteric artery
IR	Inversion recovery
IVDSA	Intravenous digital subtraction angiography
LOCM	Low-osmolar contrast materials
MALS	Median arcuate ligament syndrome
MAR	Mesenteric-aortic velocity ratio
MDCTA	Multi-detector CT angiography
MIP	Maximum intensity projection
MPR	Multi Planar reformation
MRA	Magnetic resonance angiography
MRI	Magnetic resonance imaging
MSCT	Multislice computed tomography
MV	Mean flow velocity
PC	Phase-contrast
PCA	Phase Contrast Angiography
PI	Pulsatility index
PRF	Pulse repetition frequency
PSV	peak systolic velocity
RI	Resistive index
ROI	Region of interest
SFA	Superficial femoral artery
SMA	Superior mesenteric artery
SNR	Signal-to-noise ratio
SSD	Shaded surface display
TE	Echo time

TI	Inversion time
TOF	Time-of-flight
TR	Repetition time
US	Ultrasonography
VE	Virtual endoscopy
VOI	Volume of interest
VR	Volume rendering
WI	Weighted image

List of figures

$\mathcal{N}o$	Figure	Page
1	Abdominal aorta and its major branches	8
2	Replaced right hepatic artery	10
3	Replaced common hepatic artery	10
4	The main collateral vessels in occlusion of the CA or SMA	13
5	Angiogram of the abdominal aorta and its major branches	14
6	Arterial phase DSA of the superior mesenteric artery	16
7	DUPLEX US of the celiac trunk	18
8	Normal postprandial duplex of the celiac artery	18
9	Normal blood flow in the superior mesenteric artery	19
10	Normal values of flow velocity in the SMA	20
11	Waveform pattern of aberrant hepatic artery	21
12	Origin of the Inferior mesenteric artery from the aorta	22
13	Volume rendered CT image of the mesenteric arteries	23
14	Sagittal 3D CT scan of the celiac axis and SMA	24
15	Volume-rendered image of the inferior mesenteric artery	25
16	GE-MRA image of a normal mesenteric arteries	26
17	Sagittal MRA image of CA and SMA	27
18	Mesenteric MRA showing aberrant right hepatic artery	27
19	Collateral vessels in a 79-year-old patient	31

No	Figure	Page
20	Events involved in atherosclerosis	33
21	The difference between the normal & atherosclerotic artery	34
22	Typical anatomy of the median arcuate ligament	38
23	Drawing illustrates measurements used to determine the degree of vascular stenosis	45
24	Drawings illustrate how projection images and a cross- sectional image are used to measure the diameter of an eccentric arterial stenosis	46
25	The relationship between area reduction and diameter reduction in a completely concentric stenosis	48
26	Micropuncture access set	54
27	Visceral hook, sidewinder &cobra shaped catheters	56
28	Vascular access catheters	66
29	Selective catheterization of the hepatic and gastroduodenal arteries	68
30	Selective catheterization of the left gastric artery	69
31	Aliasing in the color mode suggests a high-grade stenosis at the origin of the SMA	79
32	Upper abdominal longitudinal US scan	81
33	Schematic representation of the origin of the SMA from the aorta	84
34	Schematic representation of the origin of the IMA	85
35	Schematic illustration of a dual-source CT	90
36	Graphical demonstration of the dose-buildup effect of the radiation penumbra with 4-, 16-, and 64-slice CT	36
37	Automated exposure control: demonstration of z-axis	98

$\mathcal{N}o$	Figure	Page
	dose modulation	
38	Principle of improved z-sampling with the z-flying focal spot technique	99
39	CPR CT image through the SMA	110
40	MIP CT angiogram of the mesenteric vessels	111
41	A volume-rendered image of the abdominal aorta including the mesenteric and iliac arteries	113
42	Virtual angioscopy of the normal aorta at the level of the diaphragm	114
43	CT angiography with use of both MIP and volume rendering as complementary techniques for vascular mapping	120
44	Virtual endoscopy guided by the centerline of the vessel	137
45	Three-dimensional MR visualization techniques	137
46	Flowchart of the vessel extraction and quantification process	138
47	Interaction scenario for selection of a starting point	139
48	Prediction and correction of a new axis point in a case of significant curvature	140
49	Prediction and correction of a new axis point in a case of bifurcation	140
50	Axis of the aorta and examples of orthogonal cross sections	141
51	Active contour evolution in detection of the vessel lumen boundary	141
52	Vessel contour detection along the vessel centerline	142
53	Flow analysis with PC images	143

No	Figure	Page
54	Graph plotting flow-velocity vs time for a specific ROI in the PC image	144
55	Collateral vessels by DSA	147
56	Pancreatic arcade collateral network with CA occlusion	147
57	Superior mesenteric arteriogram shows a tortuous artery that arises from a dorsal pancreatic artery	148
58	Meandering mesenteric artery in SMA occlusion	148
59	Collateral vessels in a case of abdominal angina	149
60	IMA occlusion	149
61	DSA Follow up in Chronic Mesenteric Ischemia	150
62	Angiogram of a 28-year-old man with FMD	151
63	Takayasu arteritis in a 26-year-old woman	152
64	Normal arterial spectrum obtained with Doppler US	155
65	Schematic diagram of flow through a constriction	158
66	The increase in velocity as the blood flows through a stenosis	158
67	Duplex US findings in isolated stenosis of the CA	160
68	Median arcuate ligament syndrome	161
69	The SMA arises from the aorta at an acute angle and courses anteriorly	162
70	Duplex ultrasound versus angiography in diagnosing stenosis of the origin of the SMA	163
71	The Doppler spectrum from the distal mesenteric branches	164
72	Proximal occlusion of the SMA with refilling through the gastroduodenal and pancreaticoduodenal arteries as	165

No	Figure	Page
	demonstrated by color duplex ultrasound	
73	Color duplex shows low-resistance waveform in IMA, due to proximal obstruction at the level of SMA	166
74	Duplex scanning of SMA stent-angioplasty site with velocity spectra of > 70% stenosis	167
75	Duplex sonogram obtained in distal portion of IMA	168
76	3D CT scan demonstrates occlusion at the origins of the celiac axis and SMA	170
77	Axial MIP image demonstrating the reconstituted hepatic and splenic arteries with celiac occlusion	170
78	Panoramic 3D VR and MIP images show high-grade stenoses at the origins of the CA and SMA	171
79	CPR image through the SMA, complex calcified and soft plaque is present resulting in over 90% stenosis	172
80	MPR images allowing evaluation of vessel diameter at the stenosis and in the distal segment of the SMA	173
81	Comparison of VR, MIP, and MPR algorithms in the evaluation of heavily calcified plaques	174
82	3D VR, MIP, and CPR images show stenoses of the CA and SMA	175
83	Panoramic 3D VR image displays a bilateral external iliac arterial occlusion	175
84	CTA of celiac artery compression syndrome	176
85	Sagittal 3D CT scan demonstrates encasement of the SMA	177
86	Reconstructed CT angiogram image at two years' post operation	177
87	Follow-up multi-detector row CT angiogram	178

No	Figure	Page
88	CTA of the SMA obtained before and after stent placement	179
89	CE-MRA with MIP shows atheromatous affection of the CA	180
90	MRA of normal and occluded celiac and superior mesenteric arteries	181
91	Patient with CMA showing short occlusion of the SMA	183
92	A high-grade ostial stenosis of IMA	183
93	3-D contrast-enhanced MRA in a patient with severe CMI	184
94	3D CE MRA data set in the early arterial phase showing a high-grade stenosis of the celiac trunk	184
95	Lateral MIP of the abdominal aorta shows >50% stenosis of the CA and occlusion of the SMA	185
96	SMA occlusion in a 70-year-old woman who was evaluated with MR angiography followed by conventional angiography	185
97	Lateral MIP of the abdominal aorta in a patient who had undergone aorto-bifemoral bypass grafting	186
98	3D GE-MRA in a patient with isolated stenosis of the SMA just beyond the origin of a jejunal branch	187
99	MRA of Median arcuate ligament syndrome	188
100	Sagittal 3D MRA in a case of Takayasu arteritis	189
101	Involvement of the mesenteric arteries in a patient with Takayasu arteritis	189

List of tables

No	Table	Page
1	Important anomalies of the mesenteric arteries	9
2	Major mesenteric collateral pathways	11
3	Commonly used guidewires	55
4	Commonly used iodinated contrast agents	56
5	Discharge criteria after vascular and interventional procedure	71
6	complications after diagnostic angiographic procedures	73
7	Patient Preparation for CTA	101
8	Scanning and Reconstruction Parameters of CTA	102
9	Examples for protocols of CTA of the aorta with different generations of MDCT and vendors	103
10	Image Rendering Techniques	115
11	MR angiography sequence parameters	131

Pathology of abdominal angina (AA)

When arterial blood flow to the intestines compromised, a complicated disorder known as mesenteric ischemia occurs. This disorder is classified as either acute or chronic, depending on its clinical manifestation. The chronic form of mesenteric ischemia (CMI) is the pathophysiologic cause of the symptom of abdominal angina (AA), based on the fact that patients experience abdominal pain with increased demand for blood at the level of the splanchnic organs. This increased demand normally occurs after meals (Cademartiri et al., 2004).

Although Schnitzler first described the clinical picture of post prandial clinical pain in 1901, description of the syndrome of postprandial abdominal angina generally is attributed to Baccelli or Goodman (1918). In 1936, Dunphy recognized that this syndrome was a precursor of fatal intestinal necrosis; however, not until 1957 did Mikkelsen propose surgical treatment of occlusive mesenteric vascular disease. Shaw and Maynard reported the first transarterial thromboendarterectomy of the SMA in 1958, followed in rapid succession by Mikkelsen and Zarro in 1959 (*Aziz et al.*, 2009).